# Passive Network of Fabry-Perot based Sensors with Wavelength Multiplexing Capabilities

Maximillian A. Perez and Andrei M. Shkel

MicroSystem Laboratory, Mechanical and Aerospace Engineering
University of California, Irvine, CA, USA

## ABSTRACT

We introduce a technology for robust and low maintenance sensor networks capable of detecting micro-g accelerations in a wide frequency bandwidth (above 1,000 Hz). Sensor networks with such performance are critical for navigation, seismology, acoustic sensing, and for the health monitoring of civil structures. The approach is based on the fabrication of an array of highly sensitive accelerometers, each using a Fabry-Perot cavity with transparent passbands at specific wavelengths that allows for embedded optical detection and serialization. A unique feature of this approach is that no local power source is required for each individual sensor. Instead one global light source is used, providing an optical input signal which propagates through an optical fiber network from sensor to sensor. The information from each sensor is embedded into the transmitted light as a wavelength division multiplexed signal. We present for the first time the preliminary demonstration of a system of two linear serialized wavelength division multiplexed Fabry-Perot sensors with the potential for a less then 1.5dB through signal loss per device. The sensors are formed using an optical thin film multilayer structure that takes advantage of the natural non-uniformity in deposited thin films to allow serialization.

**Keywords:** MEMS, MOEMS, Fabry-Perot, fiber optic sensors, optical sensor network, wavelength division multiplex

## 1. INTRODUCTION

Fiber optic sensors (FOS) networks are an attractive approach for the pervasive monitoring of a wide variety of systems. FOS operate through the modulation of a light beam signal carried by an optical fiber by environmental effects in terms of its intensity, phase, frequency, polarization, spectral content, or some combination there of. It is widely reported that FOS have the advantages of being small and lightweight, immune to electromagnetic interference (EMI), passive, low power, have a wide signal bandwidth, and can be made environmentally rugged. They have been shown to be able to accurately sense many measurands including displacement, position (linear and angular), vibration, bending and torsion, acceleration, current, voltage, pressure, acoustic waves, temperature, strain and a wide variety of chemicals and biological substances.[1–3] Systems based on FOS can range over 1m to 100s of km with little change in architecture due to signal propagation range available to fiber optics.[4] The versatility and scalability of such systems have seen their practical deployment in a variety of applications.[5] Such properties are essential for monitoring highly distributed constructed infrastructure[6,7] and for military or peace keeping operations.[8] In addition, the possibility of integrated physical monitoring of communications infrastructure has homeland security and commercial implications.[9,10]

A number of FOS networks have been previously developed. The most popular are those based on the fiber bragg gratings (FBG).[11,12] FBG are composed of a series of closely space partially reflective elements (bragg gratings) lithographically embedded into an optical fiber core. Optical resonance forms a characteristic signal of intensity fringes in reflection based on the spacing of the fringes. Gratings of different spacings can be placed on different sections of the fiber to form distributed sensor nodes that response with fringes at different wavelengths. Their popularity is due partially to the relative simplicity of such systems since FBG are 'intrinsic' sensors formed inside and composed of the bulk of the optical fiber. It is also partially due to fact that optical signals from the network sensors nodes are readily multiplexed forming a wavelength division multiplexed (WDM) system.

Further author information: (Send correspondence to M.A.P.)
M.A.P.: E-mail: max.perez@uci.edu, Telephone: 1 949 824 6314
A.M.S.: E-mail: ashkel@uci.edu

Smart Structures and Materials 2006: Sensors and Smart Structures Technologies for Civil, Mechanical, and Aerospace Systems, edited by Masayoshi Tomizuka, et al., Proc. of SPIE Vol. 6174, 617417, (2006) · 0277-786X/06/$15 · doi: 10.1117/12.654951

Less explored are FOS networks based on Fabry-Perot Interferometer (FPI) sensors. FPIs are optical devices that use two parallel high reflectance plates to transmit a narrow optical fringe whose spectral location is highly dependent on the spacing between the plates. As such, they are fundamentally loss filters and cannot be easily serialized. FPI sensors can be both intrinsic (fiber Fabry-Perot Interferometers or FFPI) or 'extrinsic', being formed of a structure outside the fiber itself. In the case of conventional FPI, the node signals are not readily multiplexed in series like FBG since the FPI acts as a optical filter, removing all light outside the transmitted sense signal carrying fringe. Distributed sensor systems based on conventional FPI sensors generally require additional hardware or complicated signal processing dedicated to the multiplexing of signals or introduce the signal bandwidth limitations of time division multiplexing.[13–16]

FBG sensors are based on optical signal modulation due to the deformation of the fiber itself. Due to the high modulus of the fiber ($E \sim 100GPa$), FBG based sensors are focused on applications in strain and temperature monitoring. Such a high modulus sensing element works against the creation of inertial sensors based on FBG since high modulus bulk materials are not amenable for the creation of the high compliance suspended structures, such as is required for inertial devices. In contrast, FPI devices can be formed from compliant materials for the creation of inertial sensors, though their main limitation remain their difficulty to be linearly serialized.

Investigated is a transparent (all optical) WDM sensor system of FPI sensors in series, where the sense information is encoded onto different wavelengths of a light input. This is achieved by creating optical windows (transparent regions) or *passbands* in the spectral characteristics of the devices through which WDM signals from other devices can be passed. In this way WDM channels are formed. The optical characteristics are similar to FBG except that the FPI signal is transmitted downstream instead of reflected. This is advantageous since back-reflected signals can cause effects such as signal loss, noise, cross-talk, and pulse broadening.[4]

Such a system based on FPI sensors would be scalable and have a high potential sensitivity for both inertial sensors as well as other deformation based devices, such as pressure or acoustic sensors.[17] In addition this system would be power passive and immune to electromagnetic interference. The proposed system eliminates the complicated multiplexing hardware or signal processing required in other similar sensor network schemes by shifting the task of multiplexing to the optical structure of the sensors themselves. Sensor nodes can be potentially added or dropped from the system without additional hardware or reconfiguration. The technology is developed to be compatible with existing WDM communications hardware such that costs will scale downward with the inevitable maturation of that technology. In addition, such compatibility suggests the potential to integrate physical sensor nodes into communication networks. Furthermore, the development is applicable to the entire class of FPI sensors and implies the possibility of both the extension to different varieties of sensor systems and systems that include different sensor types.

We present for the first time the preliminary demonstration of a system of two wavelength division multiplexed FPI sensors. The devices are demonstrated in simple linear serialization coupled through free space transmission. Although designed as accelerometers, the devices are demonstrated under acoustic excitation. Each device is embedded with a transparent region exhibiting less then 1.5dB of signal loss per device. The sensors are formed using a low-loss optical thin film multilayer interference filter that provide spectrally distinct highly reflective and high transmissive regions to provide wavelength divided interferometric sensing and multiplexing regions. Taking advantage of the natural non-uniformity in deposited thin films these regions are wavelength shifted amongst the fabricated devices to allow serialization into a sensor network.

The paper is organized as follows: Section 2 describes the background of the mechanism of FPI sensor and explores its resolution as an accelerometer. Section 3 describes the FPI serialization technique. Section 4 describes the fabrication process and shows the optical characteristics of the sensors. Section 5 shows a demonstration of the multiplexing capabilities of two sensors in series.

## 2. THEORY OF FABRY-PEROT INTERFEROMETER (FPI) BASED SENSORS

A parallel plate Fabry-Perot Interferometer (FPI) is an elegant device consisting of two parallel partially-transmissive plates with highly reflective inner surfaces, whose principle of operation was conceived over a century ago.[18] These surfaces form a resonant optical cavity of which only wavelengths that match the optical resonant condition can escape and pass through the device, the operation of which is well understood.[19, 20] These

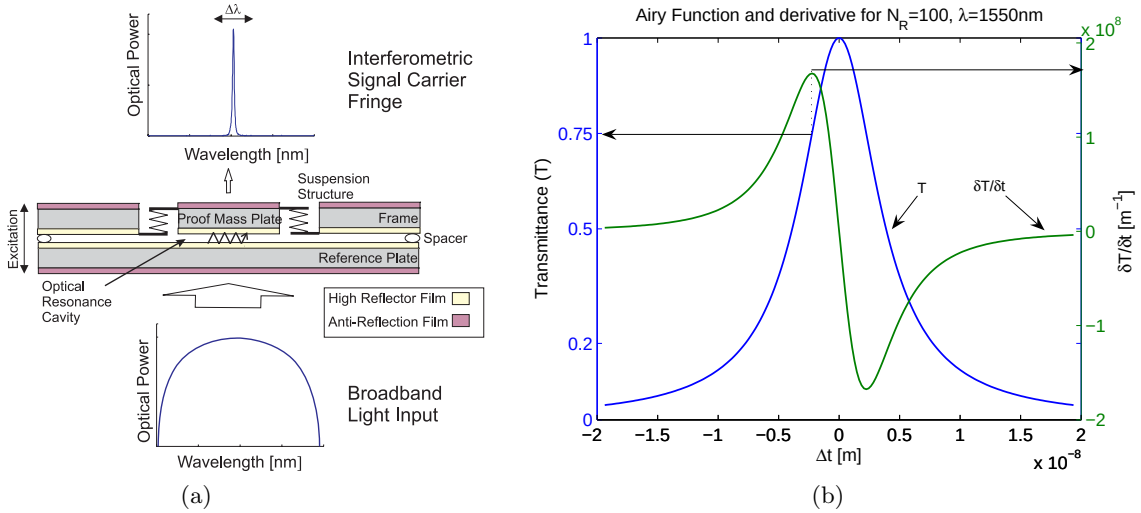


**Figure 1.** (a) FPI sensor operation as a base-excited accelerometer and (b) its optical signal characteristics in deflection of the sense plate.

devices are often thought of as optical filters which remove wavelengths of input light which do no not satisfy the resonance condition and are used extensively as such in optical communication technology.[4]

The theoretical transmittance of light of wavelength $\lambda$ through an FPI is given by the Airy function:

$$\mathcal{T} = \frac{\mathcal{T}_s^2}{(1-\mathcal{R}_s)^2}\left[1 + \frac{4\mathcal{R}_s}{(1-\mathcal{R}_s)^2}\sin^2\left(\frac{2\pi\mu t}{\lambda}\right)\right]^{-1} \tag{1}$$

for normal incident irradiance, where $\mathcal{T}_s$ and $\mathcal{R}_s$ are the transmittance and reflectance of the inner surface of the plates, respectively, and $\mu$ is the index of refraction and $t$ is the gap between the plates. Note that the *transmittance* ($\mathcal{T}$) is the ratio of transmitted to incident irradiance and, similarly, *reflectance* ($\mathcal{R}$) is the ratio of reflected to incident irradiance, where irradiance has units $[\frac{optical\ power}{area}]$. In the absence of any absorption at the inner surface, the loss coefficient $\frac{\mathcal{T}_s^2}{(1-\mathcal{R}_s)^2}$ approaches to one and $\mathcal{T}$ is unity at optical resonance. In any real device, $\mathcal{T}$ is also attenuated by losses in the bulk of the plate as well as by reflection and scattering at the outer surfaces, but these losses do not effect the shape of the Airy transmission given by Eqn. (1).

The resonance condition relating the FPI gap width to the spectral placement of it's transmittance peak, or *fringe*, is given by

$$\mu t = \frac{n\lambda}{2} \tag{2}$$

where $n$ is an integer known as the order of interference of the FPI. Eqn. (2) reduces to $t = \frac{n\lambda}{2}$ in air ($\mu_{air} \approx 1$). Commonly, MEMS-based FPI's use low orders due to micron-level plate spacing available in microsystems, but higher FPI orders maybe considered. This condition is meet at all values of $n$, and fringes may appear throughout the FPI output spectrum. Thus, the placement of the fringe determine the displacement of the sense plate of the structure and the fringe carries the sense information of sensor.

A structure such as shown in Fig. 1a takes advantage of this condition by suspending one plate relative to the other to form an accelerometer. The static response of a such a suspended mass system is defined by combining Newton's 2nd Law and Hook's Law yielding

$$a = -\frac{k}{m}\Delta t = -\omega_n^2 \Delta t \tag{3}$$

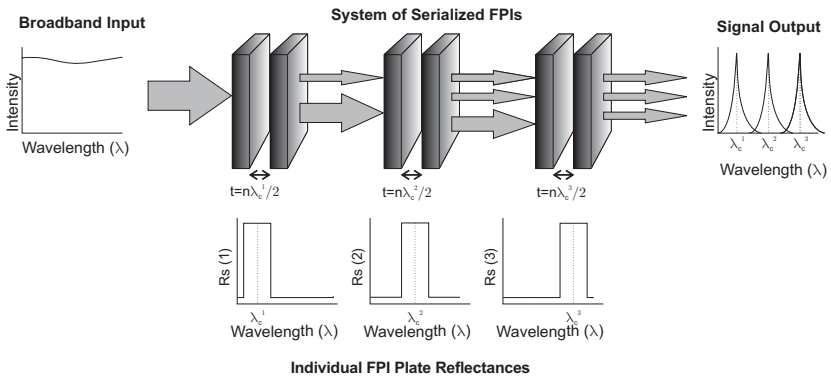


**Figure 2.** Schematic representation of an WDM system of Fabry-Perot Interferometers with device embedded multiplexing capabilities. Reprinted.[24]

This is the quasi-static relation for the deflection of a suspended plate $\Delta t$ from rest due to an acceleration, where $\omega_n$ is the angular natural frequency of the system. This relationship is generally true while the angular frequency of the acceleration is less then half of the natural frequency of the system ($\omega < \frac{1}{2}\omega_n$), which also roughly accounts for the frequency bandwidth of such a system ($\Delta f \approx 0 \rightarrow \frac{1}{2}\frac{\omega_n}{2\pi}$ Hz).[21]

A strong measure of the optical quality and usefulness of an FPI is the *finesse* (N). The finesse is the ratio of the separation of adjacent fringes (free spectral range or *FSR*) to the fringe width (full width of the fringe at half it's maximum or *FWHM*). For an FPI without defects or optical absorption, the finesse is known as the *reflectance finesse* ($N_R$), as it is related only to and increases monotonically with $\mathcal{R}_s$, and is given as

$$N_R = \frac{\pi\sqrt{\mathcal{R}_s}}{1-\mathcal{R}_s} \tag{4}$$

Commonly, commercial FPIs have actual finesse values of $N \approx 50-100$. In order to achieve a higher finesse device, both high reflectivities and fine control over plate defects and parallelism must be obtained.[22] Some tunable telecommunication FPIs using electrostatic feedback to control the parallelism of the plates have achieved finesse values up to 2000.[23]

A numerical study of the Airy function is shown in Fig. 1(b) for an FPI of the modest finesse of $N_R = 100$ where the wavelength has been fixed and the gap varied about the optical resonance point. Even with such modest a finesse, the displacement sensitivity at the Airy function's maximum slope at three-quarters transmittance is $\frac{\delta t}{\delta \mathcal{T}} = 6nm$. Assuming a FPI-based accelerometer with $f_n = 2000Hz$ and a sensor bandwidth of $1000Hz$ and assuming a couple narrowline source/photodetector detection scheme, a noise resolution as low as $2\frac{pg}{\sqrt{Hz}}$ can be calculated[17] yielding a possible acceleration resolution of better then $0.1\mu g$.

## 3. SERIALIZATION OF THE FPI SENSOR

In previous publications this group has described the general scheme for the serialization of multiple FPI sensors on a single optical line.[24,25] In general, if the plates of the FPIs are made using mirrors with blocker band or notch reflectance characteristics, optical resonance and an interferometric fringe will only occur in the narrow region of high reflectance. This region provides the signal band for that device. Light outside of this region can pass unaffected to either provide optical power for downstream sensing or to carry fringe signals from upstream sensors. Each of the network devices will have their notches in a different spectral region and produce their own fringe signal distinct from the upstream devices. These optical characteristics wavelength division multiplex the fringe signals automatically into the optical stream (Fig 2). A system operating in the well established optical C-band ($1528nm < \lambda < 1561nm$) using the ITU-I nominal wavelength channel standards ($\Delta\lambda = 0.39nm$) could support a sensor network of 81 nodes.

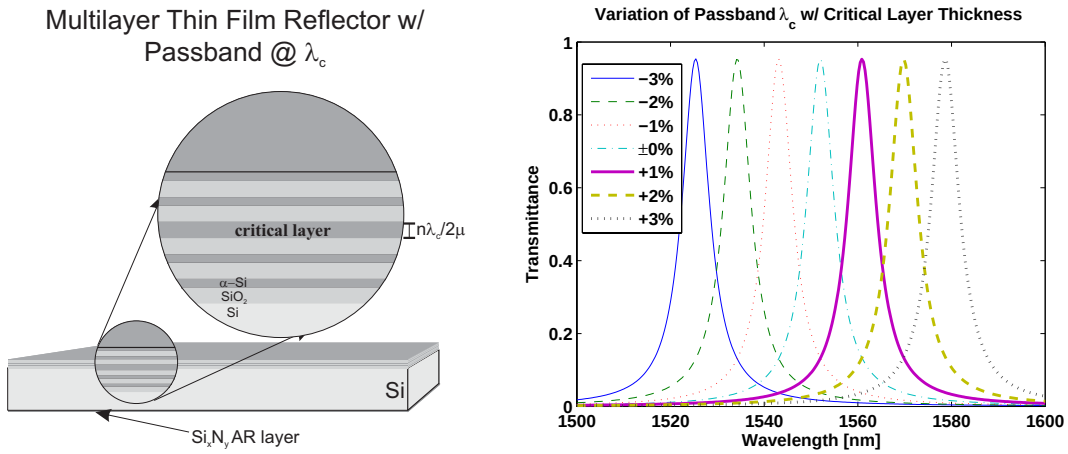


(a) (b)

**Figure 3.** (a) Structure of a thin film multilayer interference filter for the creation of optical passbands and (b) its numerically calculated (Winspall 2.20) characteristics for a $SiO_2$ and $\alpha - Si$ structure.

### 3.1. Quarter Wave Dielectric Stack Reflector

The generation of narrow band notch reflectors can be technically challenging and expensive.[25] Such structures are normally composed of alternating layers of high and low index dielectric material each of a quarter optical path thickness of the wavelength at which maximum reflectance is desired. Such layers are known as quarter-wave dielectric stacks (QWDS). Such structures are a trade off between maximum reflectance, number of layers, layer refractive index difference and blocker bandwidth.[26] A structure using QWDS suitable for the C-band system mentioned above would require layers of dielectric material separated by an index of refraction of only 0.16% (i.e. $n_L = 2.000, n_H = 2.003$). In addition, this example structure would require over 1000 precisely defined lossless layers to achieve a reflectance just approaching 0.5 suitable for a FPI sensor with a finesse of only 4.

### 3.2. Interference Filter Reflector

Alternatively, the inverse optical characteristics of those achieved by the QWDS reflector consisting of a high transmittance passband surrounded by high reflectance regions can be used to allowing the transmission of sensor network signal. While not readily generalizable to high node sensor networks, such a structure is more readily formed and can be used to study the characteristics of serial FPI WDM sensor systems. In addition, such characteristics would be useful for the integration of a single sensor into optical communications networks to allows the passage of traffic in the passband and provide integrated sensing in the sensor signal band.

Such optical characteristics are readily achieved using a thin film interference filter. An interference filter is an all dielectric 'fixed gap' FPI with a thin film acting as the 'gap' between two high reflective surfaces and is described by relationships (1), (2), and (4). The optical mulitlayer structure is formed of two QWDS separated by a half-wave thin film layer as shown in Fig. 3a. Such an optical structure forms a narrow transparent region surrounded by regions of high reflectance as in Fig. 3b. Where as the thickness of all the layers affect the placement of the blocker band in the QWDS, interference filters are unique in that the spectral placement of their transmittance fringe ($\lambda_c$) is uniquely determined by the width of the central half-wave 'gap' layer. As little as a $\pm 3\%$ variation in this layer can cause a spectral variation in placement of $\lambda_c$ of the passband to span the optical c-band.

In this work, a total of ten thin films of silicon dioxide ($SiO_2$) and amorphous silicon ($\alpha - Si$) were deposited by plasma enhanced chemical vaper deposition (PECVD) (Plasma-Therm 790) to form the interference filter on a double side polished (DSP) Si wafer, as seen in 4a. $SiO_2$ ($n \approx 1.4$) and $\alpha - Si$ ($n \approx 3.7$) are characterized by their large difference in index of refractions. Such a large difference increases the reflectance of the individual QWDS halfs increasing the quality of the transmittance fringe for a lower number of layers, both decreasing the

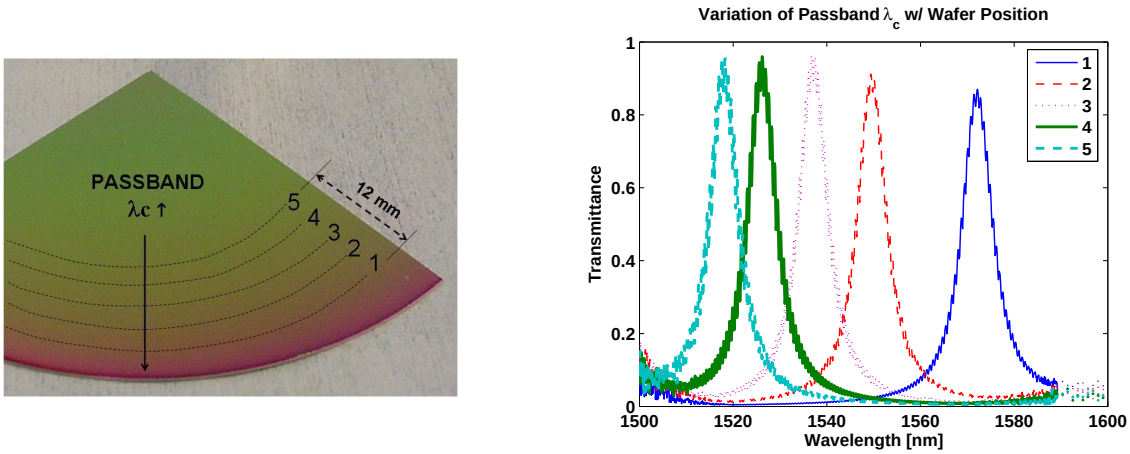


(a) (b)

**Figure 4.** (a)Location of experimental transmittance curves of (b) on the optically coated bulk wafer used for device fabrication. Note that radial color variation clearly indicates the radial dependence of thin film thickness.

passband width and passband signal insertion loss. Such large index of refraction difference are not available for other possible material systems, such as those involving the commonly used stoiciometric silicon nitride $Si_xN_y$ ($n \approx 1.8 \rightarrow 2.0$).[19]

We observe the transmittance of the passband with the maximum transmittance of each plate greater then 90% such that signal loss of less then 0.5dB is expected for transmittance through each plate at the passband peak, as shown in Fig. 4b. For transmission through two plates such as is required to create an FPI sensor, a minimum insertion loss for passed signals for each sensor node of less then 1dB is expected.

The dependence of the spectral placement of the transmittance fringes can be used to create passband regions in different parts of the sensor networks spectrum using a single wafer. Due to the differences in deposition rates that develop radially across the substrate wafer during PECVD processing due to gas flow and thermal gradients,[27] the spectral placement of the transmittance fringe is observed to have a radial symmetry with respect to testing point on the wafer as in Figs. 4a,b. Comparison between the numerically simulated response of Fig. 3b and the experimental characteristics shown in Fig. 4b indicate that the variation in the critical central $\alpha - Si$ layer is sufficient to explain the spectral passband shift radially across the wafer.

## 4. THE FPI-BASED SENSOR

### 4.1. Fabrication

Fig. 5a illustrates the steps used for the fabrication of the bulk micromachined FPI sensors. The device is fabricated by first depositing on one side of a double sided polished (DSP) wafer (1) the multilayer interference filter. On the other side, an anti-reflectance (AR) layer of stoichiometric silicon nitride ($Si_xN_y$) is deposited (2). A thick photoresist (AZ4620) layer is spun on and is lithographically patterned (3). The wafer is attached to a handel wafer via a water soluble adhesive (Crystalbond 555) and a DRIE system (STS MESC ICP Etcher) is used to through-etch the wafer from the AR surface to the QWDS surface (4). The flexure suspension structures for the proof mass plate are formed while the device wafer is still attached to the handel wafer, by depositing catalyzed liquid polymer (Dow Corning Sylgard© 184) into the etched trench via a pulled micropipette using the through-etch channels as a mold (5). This polymer is cured at room temperature overnight forming a solid, but compliment elastomer providing a well defined flexure for the proof mass. Reference plate structures are created similarly but without the elastic flexure. The devices are removed by melting the adhesive and dissolving any residual adhesive in warm water (6). The plates are assembled into FPI sensors by aligning the plates to each other while observing the transmitted interferometric fringe from a broadband source (HP 83438A)

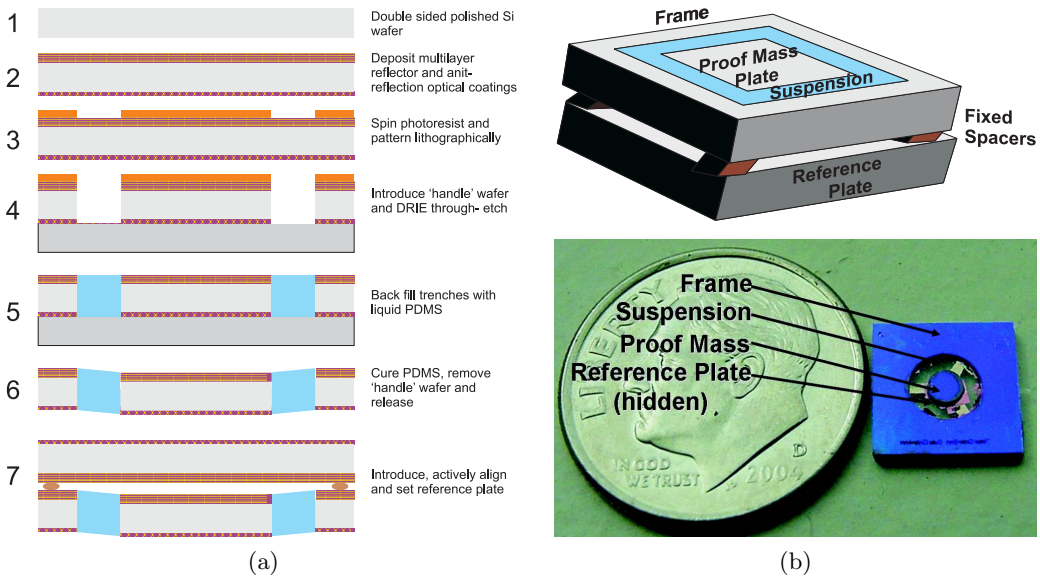


**Figure 5.** (a)Fabrication and (b)structure of an FPI accelerometer.

free space coupled to a optical spectrum analyzer (Agilent 86140B) and allowing epoxy beads to set when the interferometric fringe is at maximum finesse (7). This assembly process allows spectral position of the signal carrying fringe to be varied arbitrarily (within the limits of the process) allowing it to fall in a signal band that is wavelength aligned to the passbands of the other devices in the serial system.

The devices are fabricated to obtain passband characteristics in different regions by using a radially oriented lithographic mask. By creating devices from different sections of the wafer, different WDM passbands can be formed. Plate pairs with similar passband placements are formed by creating both proof mass and reference plate structures at the same radial distances (Fig. 6).

## 4.2. Optical Characterization

Optical characterization of the devices were achieved by passing the collimated beam from a broadband light source (HP 83438A) through each device or serial system of devices. The response was free space coupled to a optical spectrum analyzer (Agilent 86140B). The results are normalized as transmittance by dividing the through device transmitted power by the device free transmitted power.

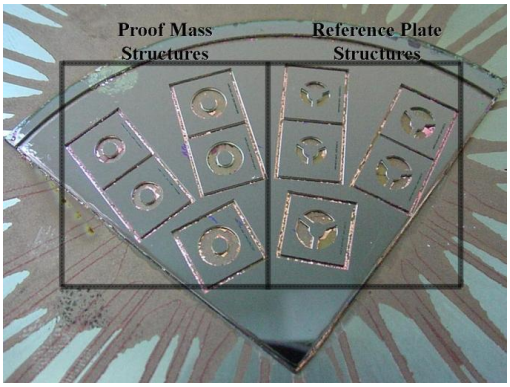


**Figure 6.** Through etch of the optically coated substrate wafer attaches to handel wafer with a radial orientation.

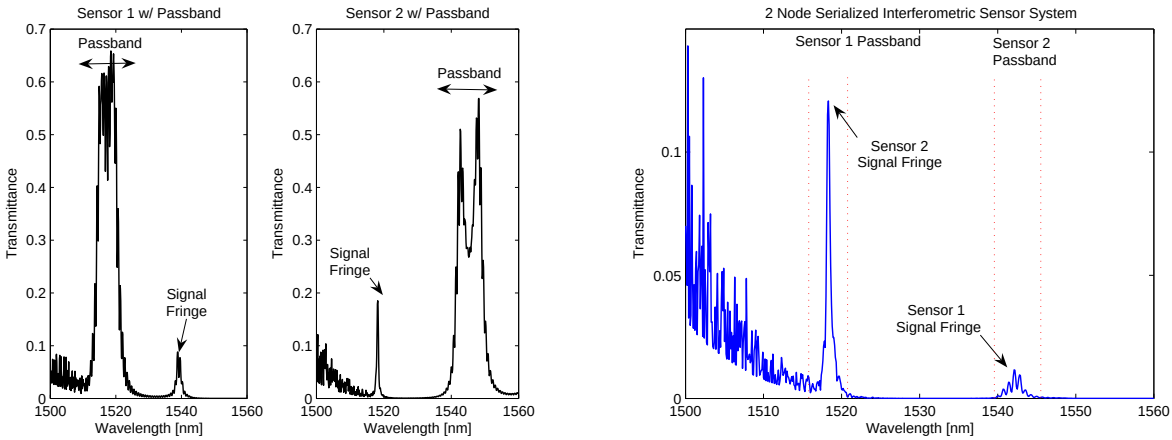


(a) (b)

**Figure 7.** Experimental optical characteristics of the (a) Individual and (b) Serialized FPI sensors

Only optical pairs of proof mass and reference plates with matching passband spectral positions are assembled in FPI sensors. When the optical properties of the interference film fringes overlay, a passband through the FPI sensor is formed (Fig. 7a). The contribution from the individual passbands from each plate is evident as spikes at its edges. This is due to the slight spectral misalignment between the passbands of each plate. Since serialized transmittance through a number of device is

$$\mathcal{T}_{total}(\lambda) = \mathcal{T}_1(\lambda) \times \mathcal{T}_2(\lambda) \times ... \tag{5}$$

spectral passband misalignment is manifested as such fringes. The signal band is formed around the FPI fringe in the highly reflective regions outside the passband. Passbands of assembled FPI sensors with maximum transmittances as high as $\mathcal{T} = 0.7$ were achieved indicating an insertion loss of passed signals of 1.5dB.

By using conjugate pairs of devices, with one device's sense fringe falling in the passband of the other, and vice-versa, the serialization of the signal fringes of the two devices can be achieved, as in Figs. 7b and 8a. Since the transmittance properties of the passbands are locked to the characteristics of the individual plates and not to the FPI gap, irregularity in the passband should not effect the sensing capabilities of the system when monitored as a modulation of transmitted optical power at a particular wavelength.

## 5. DEMONSTRATION OF A FPI SENSOR SERIALIZATION

The operation of single FPI sensors fabricated as above has been previously demonstrated and examined by this group.[28] Using similar techniques, a system of two serialized devices is demonstrated. The demonstration is achieved by directing a tunable laser (HP 8168E) through two appropriate devices with wavelength shifted transmittance characteristics in series and monitoring the transmitted power via an amplified photodetector (Thorlabs PDA255). The laser output power is fixed (1000 $\mu$W) at the -3dB wavelength of each devices fringe. Both samples are simultaneously excited acoustically via a voice coil in a sinusoidal fashion, as in Fig. 8b. As the interference fringe moves from its rest position under the load, the transmitted optical power is attenuated according to the sample's optical and mechanical characteristics. The wavelength of the laser is switched between the -3dB point of the two devices to eliminate the need for demultiplexing the wavelength signals after transmission but the orientation of the devices is not adjusted. The acoustic input power is monitored by a small condenser microphone (Radio Shack 33-3013) is manifested as a voltage. The response of each device as a optical power modulation is also monitored as a voltage from the photodetector. For the serialized system with the characteristic of Fig. 9a, Fig. 9b demonstrates the response of each sensor to the same acoustic excitation.

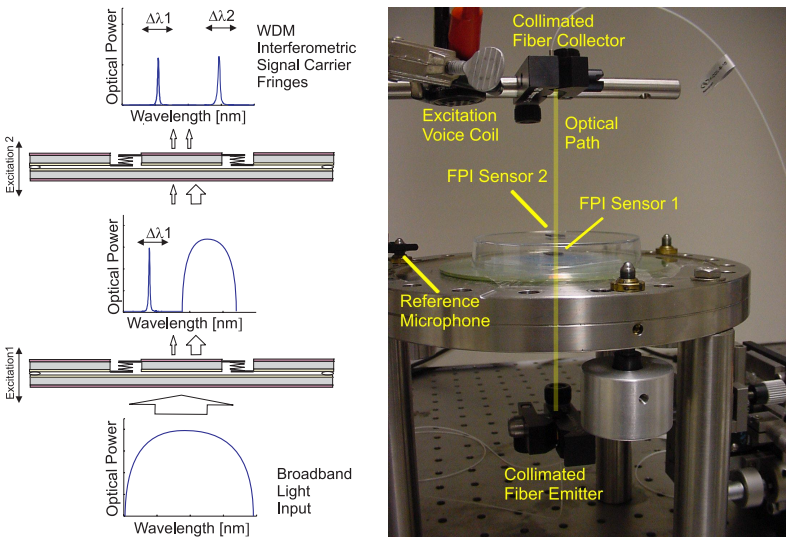


(a) (b)

**Figure 8.** (a) A system of two serialized devices with multiplexing capabilities (b) demonstrated under acoustic excitation.

## 6. CONCLUSIONS

For the first time, Fabry Perot interferometric sensors have been experimentally shown to have the potential for linear serialization in a way similar to the widely used fiber bragg grating sensors. It has been shown that optical passbands with an insertion loss less then 1.5dB can be fabricated in such sensors using surface deposited interference filters. This allows the sensors to multiplex their signals by wavelength without any additional equipment or signal processing and the complexity of the system was successfully transferred to the structure of the optical coatings of the sensors. In addition, the natural process variation in such surface deposited filters can be used to shift the wavelength placement of the passbands to allow devices fabricated from a single process to a system of serializable devices. Using this technique the linear serialization of two such sensors was achieved and a preliminary dynamic demonstration of the distributed sensor system was presented.

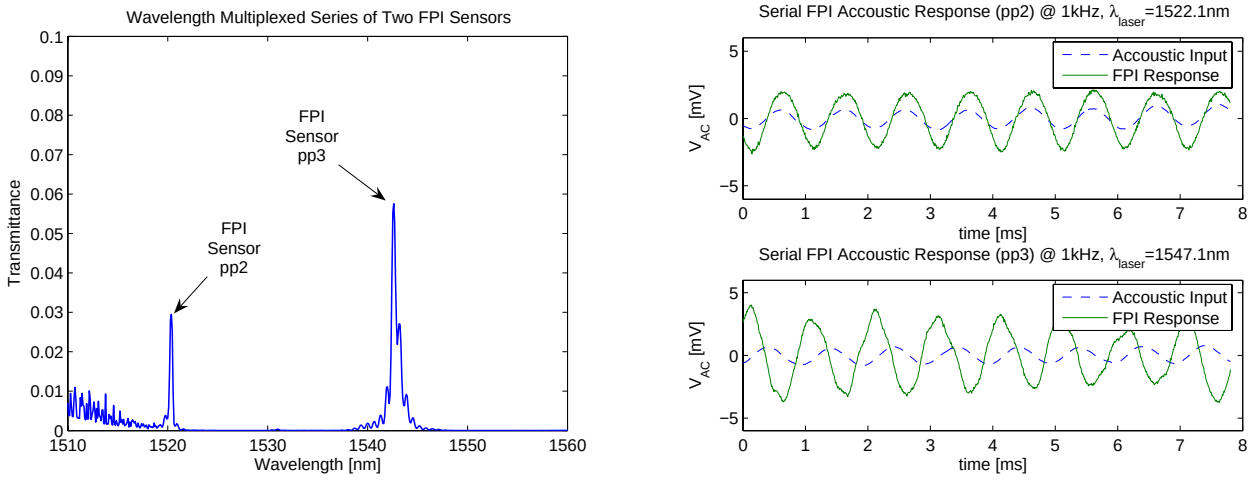


(a) (b)

**Figure 9.** (a) Demonstration of two wavelength multiplexed FPI sensors (b) under acoustic excitation.

## ACKNOWLEDGMENTS

Supported in part by the National Science Foundation Grant CMS-0330470 and by UC Discovery/VIP Sensors grant 9-442531-19919-8. Thanks due to Michael J. Little, Adam Schofield, E. Jesper Eklund and Alex Trusov for motivating discussion.

## REFERENCES

1. B. Lee, "Review of the present status of optical fiber sensors," *Optical Fiber Technology* **9**, 2002.
2. E. Udd, "Fiber optic smart structures," *Proceedings of the IEEE* **84**, pp. 884–894, June 1996.
3. O. S. Wolfbeis, "Fiber-optic chemical sensors and biosensors," *Analytical Chemistry* **76**, pp. 3269–3284, June 2004.
4. S. V. Kartalopoulos, *Introduction to DWDM Technology: Data in a Rainbow*, IEEE Press, New York, 2000.
5. C. I. Merzbacher, A. D. Kersey, and E. J. Friebele, "Fiber optic sensors in concrete structures: a review," *Smart Material and Structures* **5**, 1995.
6. K. P. Chong, N. J. Carino, and G. Washer, "Health monitoring of civil infrastructures," *Smart Materials and Structures* **12**, pp. 483–493, May 2003.
7. E. Aktan, S. Chase, D. Inman, and D. Pines, "Monitoring and managing the health of infrastructure systems," *Proceedings of the 2001 SPIE Conference on Health Monitoring of Highway Transportation Infrastructure* , 2001.
8. J. Altmann, H. Fischer, and H. Graaf, *Sensors for Peace: Applications, Systems and Legal Requirements for Monitoring in Peace Operations*, United Nations, 1998.
9. K. Poulsen, "The backhoe: A real cyberthreat," *Wired News* , 2005.
10. A. Markopoulou, G. Iannaccone, S. Bhattacharyya, C. Chauh, and C. Diot, "Characterization of failures in an ip backbone," tech. rep., Intel, 2003.
11. A. D. Kersey, T. A. Berkoff, and W. W. Morey, "Muliplexed fiber bragg grating strain-sensor system with a fiber fabry-perot wavelength filter," *Optics Letters* **18**, August 1993.
12. A. D. Kersey, M. A. Davis, H. J. Patrick, M. LeBlanc, K. P. Koo, C. G. Askins, M. A. Putnam, and E. J. Friebele, "Fiber grating sensors," *Journal of Lightwave Technology* **15**, August 1997.
13. W. Li, D. C. Abeysinghe, and J. T. Boyd, "Wavelength multiplexing of microelectormechanical system pressure and temperature sensors using fiber bragg gratings and arrayed waveguide gratings," *Society of Photo-Optical Instrumentation Engineers* **42**, pp. 431–438, February 2003.
14. M. Singh, C. J. Tuck, and G. F. Fernando, "Multiplexed optical fibre fabry-perpt sensors for strain metrology," *Smart Materials and Structures* **8**, pp. 549–553, 1999.
15. Q. Wang, "An optical fiber multiplexing system using fabry-perot cavities," *Review of Scientific Instruments* **84**(1), 1993.
16. N. Fursenau, M. Schmidt, H. Horack, W. Goetze, and W. Schmidt, "Extrinsic fabry-perot interferometer vibration and acoustic sensor systems for airport ground traffic monitoring," *IEEE Proc.-Optoelectron* **144**, June 1997.
17. E. J. Eklund and A. M. Shkel, "Factors affecting the performance of micromachined sensors based on fabryperot interferometry," *Journal of Micromechanics and Microengineering* **15**, pp. 1770–1776, July 2005.
18. C. Fabry and A. Perot, "Thorie et applications d'une nouvelle mthode de spectroscopie interfrentielle," *Ann. Chim Phys. Paris* **16**, pp. 115–144, 1899.
19. H. A. Macleod, *Thin-Film Optical Filters*, Institute of Physics Publishing, Bristol–Philadelphia, 3 ed., 2001.
20. M. Born and E. Wolf, *Princples of Optics*, Pergamon, London, 7th ed., 1999.
21. H. Eren, *Acceleration, Vibration, and Shock Measurement*, ch. 17.
22. P. D. Atherton, N. K. Reay, J. Ring, and T. R. Hicks, "Tunable fabry-perot filters," *Optical Engineering* **20**(6), pp. 806–814, 1981.
23. Solus-Micro-Technologies, "New tunable filters use compliant mems technology to deliver superior performance at lower cost in optical networking applications." Internet Press Release, March 2002.

24. M. A. Perez and A. M. Shkel, "Conceptual design and preliminary characterization of serial array system of high-resolution mems accelerometers with embedded optical detection," *Smart Structures and Systems* **1**, December 2004.
25. M. Perez, "Micromachined elastomeric accelerometers with embedded optical detection for serial sensor networks," Master's thesis, University of California, Irvine, 2004.
26. R. R. Willey, "Estimating the number of layers required and other properties of blocker and dichroic optical thin films," *Applied Optics* **35**, pp. 4982–4986, September 1996.
27. J. Foggiato, *Handbook of Thin Film Deposition*, ch. 3. Noyes, 2002.
28. M. A. Perez, E. J. Eklind, and A. M. Shkel, "Designing micromachined accelerometers with interferometric detection," *IEEE Sensors 2005 Conference Proceedings* , 2005.